

## Photoluminescent silicon nanocrystals synthesized by reactive laser ablation

Daria Riabinina,<sup>a)</sup> Christophe Durand, Mohamed Chaker,<sup>a)</sup> and Federico Rosei  
 INRS-EMT, Université du Québec, 1650 Lionel-Boulet, Case Postale 1020, Varennes Qc J3X 1S2, Canada

(Received 24 August 2005; accepted 22 December 2005; published online 15 February 2006)

We report the synthesis of Si nanocrystals embedded in a SiO<sub>2</sub> matrix using reactive laser ablation in oxygen atmosphere followed by annealing. We observe a strong photoluminescence signal, which is related to the oxygen background pressure used for synthesis. The average nanoparticle size, obtained independently by fitting photoluminescence spectra and from x-ray diffraction patterns, decreases from 16 to 2 nm with increasing oxygen pressure from 0.01 to 1.1 mTorr. The maximum photoluminescence intensity is observed at 0.8 mTorr, which corresponds to a crystal size of 2.2±0.4 nm. We find that the concentration of nonoxidized Si, which is controlled by the oxygen pressure, determines the final nanocrystal size. © 2006 American Institute of Physics. [DOI: 10.1063/1.2174096]

Light emission due to quantum confinement in semiconductor nanostructures<sup>1,2</sup> is a remarkable phenomenon in fundamental physics that has recently attracted great interest due to its potential applications in Si-based optoelectronic devices.<sup>3–6</sup> Different types of Si nanostructures have been synthesized by various methods, including ion implantation, laser ablation, sputtering, etc.<sup>7–10</sup> The main difficulties related with the synthesis of interesting Si nanostructures so far are the nonuniform size distribution, the low density of nanoparticles, the low photoluminescent efficiency, and the limited size control.

Pulsed laser deposition (PLD) is a versatile technique for the growth of thin films and nanostructured materials. The variation of deposition kinetic energy yields significant changes in film properties.<sup>11</sup> For example, it has been demonstrated that PLD of semiconductors in an inert gas atmosphere allows the synthesis of photoluminescent nanoparticles with controlled size.<sup>7,12,13</sup>

Laser ablation in a reactive gas atmosphere (also called reactive PLD) is a powerful method to control the stoichiometry of deposited films. The optical properties of SiO<sub>2</sub> thin films deposited under oxygen pressure have recently been investigated for optoelectronic applications such as waveguides.<sup>14,15</sup> The formation of P- and Er-doped Si nanoparticles by PLD has also been explored.<sup>16,17</sup> However, the influence of the oxygen background pressure on the formation of Si nanocrystals remains so far unexplored.

In this letter, we report the synthesis of Si nanocrystals embedded in a SiO<sub>2</sub> matrix using reactive laser ablation in an oxygen background atmosphere. SiO<sub>x</sub> films (0 ≤ x ≤ 2) were deposited on Si substrates covered with native oxide by conventional PLD under low oxygen pressure (0.01–1.5 mTorr). A Si rotating target (undoped Si wafer) was ablated by using a pulsed excimer KrF laser (λ = 248 nm) with a pulse duration of 17 ns and a repetition rate of 20 Hz. The laser fluence was set at 5 J/cm<sup>2</sup> and the substrate-target distance maintained at 40 mm. The thickness of the deposited films was ~200 nm, as measured by imaging the sample section by scanning electron microscopy. Af-

ter deposition in the oxygen atmosphere, the SiO<sub>x</sub> films were annealed for 1 h at 1050 °C in an inert gas atmosphere (N<sub>2</sub>). The structural and optical properties of the deposited films have been studied by x-ray diffraction (XRD), x-ray photoelectron spectroscopy (XPS), and photoluminescence spectroscopy (PL). The PL spectra of the samples were measured at room temperature, using a diode laser (405 nm, 25 mW) for the photonic excitation.

Figure 1 displays PL spectra for samples deposited for six values of oxygen pressure ranging from 0.26 to 1.5 mTorr. The inset of Fig. 1 shows the variation (for 0.68 mTorr) of a PL spectrum as a function of laser excitation power. These changes can be associated with the change of the distribution of excited carriers (obtained by increasing the excitation power) between energy levels in the zero-dimensional quantum-confined structures. We note that the PL intensity increases with the oxygen pressure increase between 0.26 and 0.8 mTorr. This increase, which is well correlated with the reduction of nanocrystal size (as discussed later), is attributed to the increase of the oscillator strength and to the decrease of non-radiative Auger recombination processes as the crystal size decreases.<sup>18,19</sup> A further pressure increase in oxygen pressure (to 1.1 mTorr) results in a decrease of the PL signal. This effect could be explained by a low density of Si nanocrystals and/or by the low absorbance of excitation light for this sample.

The position and shape of PL spectra depend on nanocrystal size and size distribution. The position of PL peaks can be determined by solving the Schrödinger equation for a zero-dimensional quantum structure

$$\Delta E = \frac{h^2}{8mr^2}i^2, \quad i = 1, 2, 3, \dots, \quad (1)$$

where the electron state energy above the band gap is  $\Delta E = h\nu - E_g$  with recombination energy  $h\nu$ , Si band gap  $E_g = 1.14$  eV,<sup>20</sup> effective mass  $m = 0.155m_0$ , free electron mass  $m_0$ , nanoparticle size  $r$ , Planck constant  $h$ , and quantum number  $i$ . Assuming a Gaussian distribution for the nanoparticle size  $r$ ,<sup>21</sup> the shape of PL spectra can be calculated by using the relation<sup>22,23</sup>

<sup>a)</sup> Authors to whom correspondence should be addressed; electronic mail: riabinina@emt.inrs.ca and chaker@emt.inrs.ca

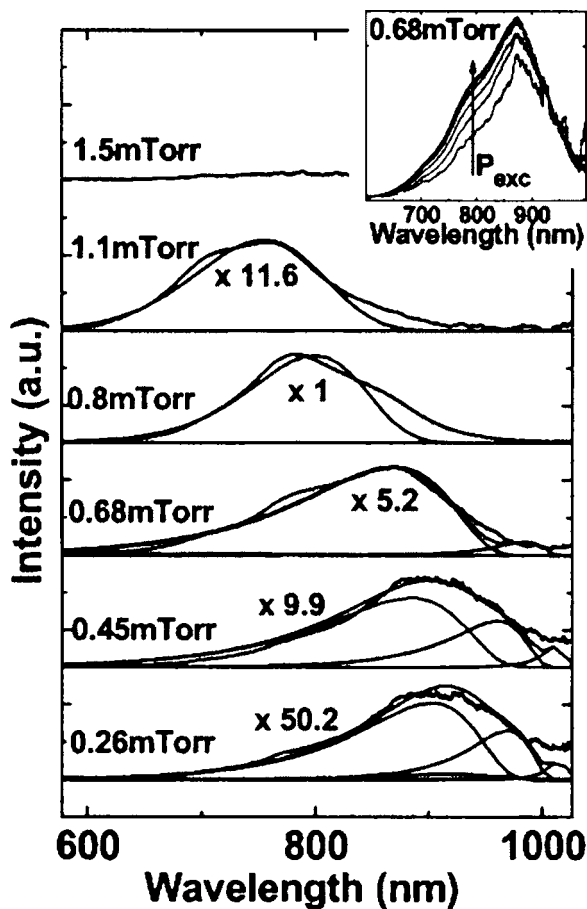


FIG. 1. Photoluminescence spectra of Si nanocrystals as a function of oxygen pressure. All the PL spectra were normalized and the scaling factors are indicated in the figure. In the inset, we display the normalized PL spectrum of the sample deposited under 0.68 mTorr as a function of excitation power from 0.5 to 25 mW.

$$P(\Delta E) \propto \frac{nC^2}{2\sigma\sqrt{2\pi}(\Delta E)^3} \exp\left\{-\frac{1}{2}\left(\frac{r_0}{\sigma}\right)^2\left[\left(\frac{\Delta E_0}{\Delta E}\right)^{1/2} - 1\right]^2\right\} \quad (2)$$

with the number of nanocrystals  $n$ , mean nanocrystal radius  $r_0$ , coefficient  $C = h^2 v^2 / 8m$ , and  $\Delta E_0 = C/r_0^2$ . Thus, Eq. (2) establishes a correlation between the shape of PL spectra and the size  $r$  with size distribution  $\sigma$  of nanoparticles. Using Eq. (2), we fitted the PL spectra of Si nanoparticles in the samples deposited under various oxygen pressures by varying the size  $r_0$  and the size distribution  $\sigma$ . Table I reports the size of Si nanoparticles calculated from fits of PL spectra.

To gain further insight on the significant PL signal observed, which occurs only in the specific O<sub>2</sub> pressure range

TABLE I. Si nanocrystal size calculated from simulations of PL spectra.

Oxygen pressure (mTorr)	Nanoparticle size $r_0$ (nm)	Size distribution $\sigma$ (nm)
1.1	1.9(±0.1)	0.2(±0.03)
0.8	2.2(±0.1)	0.4(±0.03)
0.68	3.6(±0.1)	1.8(±0.1)
0.45	5.3(±0.2)	3(±0.1)
0.26	6.5(±0.2)	3(±0.1)

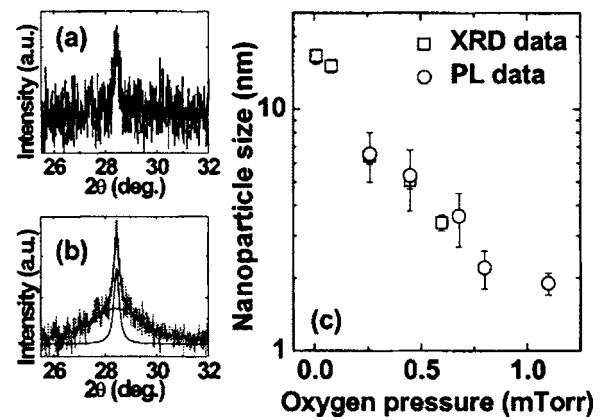


FIG. 2. XRD analysis of Si nanocrystals: (a) (111) XRD peak of as-deposited samples (0.68 mTorr); (b) (111) XRD peak of annealed samples deposited under 0.68 mTorr; and (c) nanocrystal size calculated from the broadening of (111) XRD peak as a function of oxygen pressure.

0.26–1.1 mTorr, we performed structural and chemical characterization by using both XRD and XPS.

It is well known that PLD produces films with micron sized particles (also called droplets).<sup>24</sup> Their origin is intrinsic to the laser ablation process. The as-deposited XRD pattern yields a peak whose full width half maximum (FWHM) is equal to the diffractometer resolution (0.2°). Thus the narrowness of the XRD pattern of the as-deposited samples [Fig. 2(a)] showing the (111) peak of Si is due to the dominance of droplets in the film. As shown in Fig. 2(b), after annealing, an additional wide peak with FWHM equal to 2.67° is superimposed on the XRD pattern. The broadening of the XRD peak is naturally associated with the formation of Si nanocrystals. Assuming the absence of nonuniform strain in these Si nanocrystals, we estimated the nanocrystal size from XRD patterns for various oxygen pressures with spectra such as that of Fig. 2(b). These nanocrystal sizes were displayed in Fig. 2(c), together with the nanocrystal sizes extracted from PL spectral fits (Table I). The good agreement shown in Fig. 2(c) between the nanocrystal sizes calculated from PL and from the XRD data supports our fits of the PL spectra. Note that the nanocrystal size decreases exponentially from 17 to 1.9 nm with increasing oxygen pressure (in the region 0.01–1.1 mTorr).

XPS spectra were also acquired from the as-deposited samples.<sup>25</sup> The Si 2*p* XPS signal (inset of Fig. 3) is a convolution of the nonoxidized silicon peak (denoted Si<sup>0</sup>) and the oxidized silicon peaks (denoted Si–O), composed of four contributions corresponding to the Si<sup>1+</sup>, Si<sup>2+</sup>, Si<sup>3+</sup>, and Si<sup>4+</sup> oxidation states. To fit the Si 2*p* region, the relative positions of all Si contributions were taken from the literature<sup>26</sup> and were held constant for all oxygen pressures. From this fit, we can extract the relative concentration of nonoxidized Si in the sample, which is directly proportional to the ratio between the Si<sup>0</sup> peak area and the whole Si 2*p* area. Figure 3 shows the Si nanocrystal size as a function of relative concentration of nonoxidized Si. This dependence has various trends in different regions of relative concentration of Si<sup>0</sup>. For high Si<sup>0</sup> relative concentration (>50%), i.e., low oxygen pressure (0.01–0.08 mTorr), the nanocrystal size is ~16 nm. This constant size is attributed to the formation of crystal grains in accordance with activation energies typical of bulk diffusion.<sup>27</sup> Consequently, the final grain size formed

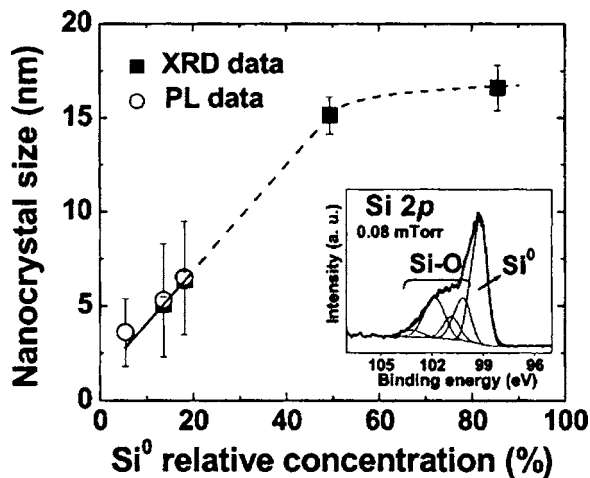


FIG. 3. Si nanocrystal size calculated from XRD and PL data as a function of the ratio “nonoxidized Si/total Si” obtained by XPS analysis in as-deposited films. In the inset, an example of Si 2*p* peak deconvolution onto nonoxidized (Si<sup>0</sup>) and oxidized (Si–O) components (sample deposited under 0.08 mTorr).

after annealing depends on the temperature and the time of annealing.

As the pressure increases from 0.08 to 1.1 mTorr, the Si<sup>0</sup> relative concentration decreases from 50% to 5%. In this region, the size of nanocrystals seems to be directly proportional to the amount of non-oxidized silicon. When the Si<sup>0</sup> concentration is close to zero, the nanocrystal is mainly composed of silicon sub-oxides (Si<sup>1+</sup>, Si<sup>2+</sup>, and Si<sup>3+</sup>). This could explain why the linear fit (Fig. 3) gives a nonzero *y* intercept and thus a nanocrystal size even when the Si<sup>0</sup> concentration is equal to zero. This XPS analysis demonstrates that for our conditions the nonoxidized Si concentration is the key parameter that determines the size of Si nanocrystals in the range of 0.08–1.1 mTorr of oxygen pressure (i.e., below 50% of Si<sup>0</sup>).

In conclusion, we produced photoluminescent Si nanocrystals embedded in a SiO<sub>2</sub> matrix using reactive laser ablation followed by a postannealing treatment. We demonstrated that the nanocrystal size can be directly controlled by the oxygen background pressure in the ablation process. A size reduction down to 2.2±0.4 nm (as measured by PL and XRD) was observed by increasing the oxygen pressure from 0.01 to 0.8 mTorr. This size reduction strongly enhances the PL intensity. The initial nonoxidized Si concentration in the as-deposited films, which is directly related to the oxygen pressure, determines the nanocrystal size. This allows controlling the luminescence intensity and tuning the PL spectral maximum position.

F.R. and M.C. acknowledge financial support from NSERC (Canada), FQRNT (Province of Quebec), and are grateful to the Canada Research Chairs program for partial salary support. The authors are grateful to G. G. Ross for useful discussions and use of PL equipment. They acknowledge T. W. Johnston for helpful discussions and for a critical reading of the manuscript.

<sup>1</sup>A. P. Alivisatos, *Science* **271**, 933 (1996).

<sup>2</sup>P. Lever, H. H. Tan, and C. Jagadish, *J. Appl. Phys.* **95**, 5710 (2004).

<sup>3</sup>L. Canham, *Appl. Phys. Lett.* **57**, 1046 (1990).

<sup>4</sup>J. L. Heinrich, C. L. Cutris, G. M. Credo, K. L. Kavanach, and M. J. Sailor, *Science* **255**, 66 (1992).

<sup>5</sup>L. Pavesi, L. Dal Negro, C. Mazzoleni, G. Franzo, and F. Priolo, *Nature (London)* **408**, 440 (2000).

<sup>6</sup>F. Rosei, *J. Phys.: Condens. Matter* **14**, S1373 (2004).

<sup>7</sup>A. V. Kabashin, J.-P. Sylvestre, S. Patskovsky, and M. Meunier, *J. Appl. Phys.* **91**, 3248 (2002).

<sup>8</sup>G. Franzo, F. Iacona, C. Spinella, S. Cammarata, and M. G. Grimbaldi, *Mater. Sci. Eng., B* **69**, 454 (2000).

<sup>9</sup>R. Smirani, F. Martin, G. Abel, Y. Q. Wang, and G. G. Ross, *Nanotechnology* **16**, 32 (2005).

<sup>10</sup>A. Mimura, M. Fujii, S. Hayashi, D. Kovalev, and F. Koch, *Phys. Rev. B* **62**, 12625 (2000).

<sup>11</sup>E. Irissou, B. Le Droff, M. Chaker, and D. Guay, *Appl. Phys. Lett.* **80**, 1716 (2002).

<sup>12</sup>L. Patrone, D. Nelson, V. I. Safarov, M. Sentis, and W. Marine, *J. Appl. Phys.* **87**, 3829 (2000).

<sup>13</sup>T. Seto, T. Orii, M. Hirasawa, and N. Aya, *Thin Solid Films* **437**, 230 (2003).

<sup>14</sup>A. P. Caricato, M. De Sario, M. Fernandez, G. Leggieri, A. Luches, M. Martino, and F. Prudeniano, *Appl. Surf. Sci.* **197**, 458 (2002).

<sup>15</sup>A. Masuda, S. Usui, Y. Yamanaka, Y. Yonezawa, T. Minamikawa, M. Suzuki, A. Morimoto, M. Kumeda, and T. Shimizu, *Thin Solid Films* **416**, 106 (2002).

<sup>16</sup>C. Li, K. Kondo, T. Makimura, and K. Murakami, *Appl. Surf. Sci.* **197**, 607 (2002).

<sup>17</sup>T. Makimura, Y. Yamamoto, S. Mitani, T. Mizuta, C. Q. Li, D. Takeuchi, and K. Murakami, *Appl. Surf. Sci.* **197**, 670 (2002).

<sup>18</sup>B. Delley and E. F. Steigmeier, *Phys. Rev. B* **47**, 1397 (1993).

<sup>19</sup>L. E. Brus, P. F. Szajowski, W. L. Wilson, T. D. Harris, S. Schuppler, and P. H. Citrin, *J. Am. Chem. Soc.* **117**, 2915 (1995).

<sup>20</sup>T. Takanaga and K. Takeda, *Phys. Rev. B* **46**, 15578 (1992).

<sup>21</sup>The Gaussian distribution gives a good description of a large number of nanoparticles at equilibrium (after annealing). It was demonstrated before that the distribution of Si nanocrystals can be described as a log-normal function [Y. Kanemitsu, T. Ogawa, K. Shiraishi, and K. Takeda, *Phys. Rev. B* **48**, 4883 (1993); Y. Kanemitsu, *Phys. Rep.* **263**, 1 (1995)]. For small nanocrystal size (<10 nm), this function is close to the Gaussian distribution.

<sup>22</sup>X. Chen, J. Zhao, G. Wang, and X. Shen, *Phys. Lett. A* **212**, 285 (1996).

<sup>23</sup>P. F. Trwoga, A. J. Kenyon, and C. W. Pitt, *J. Appl. Phys.* **83**, 3789 (1998).

<sup>24</sup>E. Van de Riet, C. J. C. M. Nillesen, and J. Dieleman, *J. Appl. Phys.* **74**, 2008 (1993).

<sup>25</sup>The surface of the samples was sputtered with Ar<sup>+</sup> ion beam in order to remove the native oxide and organic contamination.

<sup>26</sup>M. L. Green, E. P. Gusev, R. Degraeve, and E. L. Garfunkel, *J. Appl. Phys.* **90**, 2057 (2001).

<sup>27</sup>J. A. Thornton, *J. Vac. Sci. Technol. A* **4**, 3059 (1986).